Available online at www.sciencedirect.com

SciVerse ScienceDirect

Ceramics International 39 (2013) 7895–7902

CERAMICS INTERNATIONAL

www.elsevier.com/locate/ceramint

The enhanced bactericidal effect of plasma sprayed zinc-modified calcium silicate coating by the addition of silver

Kai Li, Youtao Xie, Haiyong Ao, Liping Huang, Heng Ji, Xuebin Zheng*

Key Laboratory of Inorganic Coating Materials, Shanghai Institute of Ceramics, Chinese Academy of Sciences, 1295 Dingxi Road, Shanghai 200050, PR China

Received 9 January 2013; received in revised form 28 February 2013; accepted 14 March 2013
Available online 22 March 2013

Abstract

Our previous work demonstrated the antibacterial activity of plasma sprayed zinc-modified calcium silicate coating. To enhance the bactericidal effect, in this paper, silver and zinc co-incorporated calcium silicate coating (ZC0.3-Ag) was fabricated onto Ti–6Al–4V substrate via plasma spraying technology. The coating was characterized by X-ray diffraction (XRD), scanning electron microscopy (SEM) and X-ray photoelectron spectroscopy (XPS) measurements. Transmission electron microscopy (TEM) showed that the silver nanoparticles 10–100 nm in diameter were randomly distributed in the amorphous matrix after the silver modification. In chemical durability test, the ZC0.3-Ag coating presented improved chemical stability when compared with that of the original and Ag-doped coating. In vitro antibacterial study indicated that the inactivation of bacteria (*Staphylococcus aureus* and *Escherichia coli*) on the ZC0.3-Ag coating was significantly enhanced compared to that on the Zn-modified coatings. The enhanced bactericidal activity was attributed to the addition of silver. Cytocompatibility evaluation demonstrated that the ZC0.3-Ag coating surface supported the adhesion and spreading of human mesenchymal stem cells (hMSCs), and no significant cytotoxicity was observed for the coating.

Keywords: B. Electron microscopy; D. Silicate; E. Biomedical applications; Bactericidal property

1. Introduction

Implant-associated infections are one of the most common and serious complications in orthopedic surgery. It is known that such infections are caused by the adhesion and colonization of bacteria on the artificial implant or the tissues adjacent to the implant surface [1,2]. An ideal approach to deter implant-associated infections would be the prevention of bacterial colonization directly at the site of implantation [3]. Recently, significant efforts have been made to develop surface properties that can inhibit bacterial colonization, and thus antibacterial surface coatings have received considerable attention [4,5].

Silver is a very strong bactericide and has received a great deal of attention because of its other benefits such as its broad antibacterial spectrum and smaller potential to develop resistant bacterial strains [6]. Recently, silver has been extensively studied as an additive to endow biomaterials with antibacterial activity. Chen et al. reported a plasma spray method to create a multifunctional hydroxyapatite (HA) coating containing silver with excellent antibacterial activity [7]. Silver-polysaccharide nanocomposite coatings were effective in killing both Gram-positive and Gram-negative bacterial strains [8]. Zheng et al. added elemental Ag to Ti–Ni alloy by means of arc melting under vacuum to introduce antibacterial activity [9]. Therefore, silver loaded biomaterials are promising biomaterials for decreasing implant-associated infections.

Our previous studies have shown that the Zn-modified calcium silicate coating ($Ca_2ZnSi_2O_7$) was found to inhibit the growth of *E. coli* and *S. aureus* on its surface, and the antibacterial mechanism was also previously discussed [10,11]. This paper builds on the previous work and concentrates on further enhancing the bactericidal activity of the Zn-modified coating by the addition of silver. The co-incorporation of zinc and silver into the calcium silicate coating possesses several advantages over either silver-doped or zinc-doped coating. First, it has been reported that the incorporation of zinc enhanced the chemical durability of the calcium silicate coating [10]. Second, the silver ion has no stimulating effect on human bone cells, although its bactericidal and anti-inflammatory activities have been extensively reported.

*Corresponding author. Tel./fax: +86 21 52414104.
E-mail address: xbzheng@mail.sic.ac.cn (X. Zheng).

0272-8842/$ - see front matter © 2013 Elsevier Ltd and Techna Group S.r.l. All rights reserved.
http://dx.doi.org/10.1016/j.ceramint.2013.03.051

However, zinc can stimulate bone growth in low concentrations [12]. So, synthesized materials containing both metal ions have premier medical interests in contrast with Ag-doped ones. Third, employing an inexpensive metal ion, i.e., zinc, instead of silver may provide economic benefits. Finally, it has been reported that silver has synergistic antibacterial activities with other antibacterial metal ions such as zinc and copper [13]. Therefore, using low concentration of both metal ions may increase the bactericidal activity of the coating and minimize the potential cytotoxicity of silver.

In the present study, Zn and Ag co-incorporated calcium silicate coating was fabricated on the Ti–6Al–4V substrate via plasma spraying. The objective of this study was to investigate the effects of silver addition on the chemical durability, antimicrobial activity and cytocompatibility of the as-sprayed coating.

2. Materials and methods

2.1. Coating preparation and characterization

Zn and Ag co-incorporated calcium silicate ceramic powders were synthesized by the sol–gel method, using calcium nitrate tetrahydrate ($Ca(NO_3)_2 \cdot 4H_2O$, SCRC, China), zinc nitrate hexahydrate ($Zn(NO_3)_2 \cdot 6H_2O$, SCRC, China), silver nitrate ($AgNO_3$, SCRC, China), and tetraethyl orthosilicate ($(C_2H_5O)_4Si$, TEOS, SCRC, China) as precursors. During the preparation process, the mol ratio of $Zn(NO_3)_2 \cdot 6H_2O$: $Ca(NO_3)_2 \cdot 4H_2O$: $(C_2H_5O)_4Si$ was maintained at 0.3: 1: 1, and 2 wt% $AgNO_3$ was added. An atmosphere plasma spraying (APS) system (F4-MB, Sulzer Metco, Switzerland) was employed to fabricate the Zn and Ag co-incorporated coating, denoted as the ZC0.3-Ag coating. Pure $CaSiO_3$ coating and $CaSiO_3$ coating doped with the same silver content as the ZC0.3-Ag coating, denoted as $CaSiO_3$-Ag coating, were also prepared and were used as the controls in the chemical durability test. The detailed procedures for the preparation of the powders and coatings are described in our previous study [10]. The phase composition of the as-sprayed coating was measured using an X-ray diffractometer (XRD, D/max 2500 V, Rigiku, Japan). The coating surface morphology was observed by field emission scanning electron microscopy (FE-SEM, JSM-6700, JEOL, Japan). The microstructure and elemental composition of the coating were analyzed by FE-TEM (JEM-2100F, JEOL, Japan) with electron probe X-ray microanalysis (EPMA, JXA-8100, JEOL, Japan). The XPS (MICRO-LAB 310F, Thermo Scientific, UK) analysis was performed using mono Mg Kα radiation at a vacuum pressure of 10-10 bar, at 15 kV and 10 mA.

2.2. Chemical durability and Ag^+ release tests

To evaluate the chemical durability and the Ag^+ release of the ZC0.3-Ag coating, the specimens were immersed in 50 ml of Tris-HCl buffer solution. The mass losses of the coatings were measured with immersion time. The released Ag^+ concentration in the solution was determined by inductively coupled plasma atomic emission spectroscopy (ICP-AES, Vista AX, Varian, USA).

2.3. Antibacterial assessment

Staphylococcus aureus (*S. aureus*) and *Escherichia coli* bacteria were each grown overnight and then suspended and diluted to 4×10^6 colony forming units per ml (CFU/ml) with sterilized water. To evaluate the antibacterial activity of the as-sprayed coating, the plate-counting method was used as described by Chen, et al. [7] Uncoated Ti–6Al–4V was employed as the control.

2.4. In vitro cell culture and cell morphology

The hMSCs were maintained in α-minimal essential medium (α-MEM, Gibco, USA) supplemented with 10% fetalbovine serum (FBS, Gibco, USA), 100 U/ml of penicillin and 100 mg/ml of streptomycin. The cells were then sub-cultured every 2–3 days using 0.2% trypsin plus 0.02% EDTA in a phosphate buffer solution (PBS).

To investigate the morphology of the hMSCs adhesion, the cells were cultured on the coating surface at a density of 4×10^4 cells/cm^2 and incubated in α-MEM culture medium supplemented with 10% FBS at 37 °C. After 24 h of incubation, the specimens were removed and rinsed with PBS to remove the unattached cells. As described in our previous work, the specimens were fixed with a 2.5% glutaraldehyde solution and then washed with 0.1 M PBS, followed by dehydration in serial graded ethanol (50%, 70%, 90% and 100%). Scanning electron microscope (SEM, S-4800, Hitachi, Japan) was employed to observe the cell morphology on the coating surfaces. Uncoated Ti–6Al–4V served as a control.

2.5. Cytotoxicity test

The cytotoxicity test was carried out according to the ISO/EN 10993-5 standard. The original extract of the ZC0.3-Ag coating was prepared by soaking the coating in α-MEM for 1 day at a ratio of 2 cm^2/ml (specimen to medium). After incubation at 37 °C for 24 h, the culture medium containing ionic dissolution products of the ZC0.3-Ag coating was collected. Then the extracts were serially diluted (1.00, 0.500 and 0.250 cm^2/ml) using serum-free α-MEM and were sterilized through filtration (0.22 μm). The hMSCs were seeded into 96-well plates at a density of 10^4 cells/cm^2 and incubated for 24 h, after which the culture medium was removed and replaced by 50 μl of α-MEM supplemented with 10% FBS and 50 μl of the appropriate concentration extracts. After 24 h of incubation, 10 μl of 3-(4,5-dimethylthiazol-2-yl)-2,5-diphenyltetrazolium bromide (MTS, Huamei Biochem, Shanghai, China) was added and incubated for 4 h. The absorbance was measured at 490 nm by a microplate reader (SPECTRA MAX PLUS 384 MK3, Thermo, USA). Uncoated Ti–6Al–4V and a cell-free blank served as the controls.

2.6. Statistical analysis

The results were expressed as the mean ± standard deviation (SD) for all experiments and were analyzed using a one-way

ANOVA with a post-hoc test. A p-value < 0.05 was considered to be statistically significant.

3. Results

3.1. Coating characterization

As shown in Fig. 1, the XRD pattern of the as-sprayed ZC0.3-Ag coating showed main peaks for the $Ca_2ZnSi_2O_7$ and Ag phases along with low-intensity and broad peaks ascribed to the $CaSiO_3$ phase. An SEM micrograph of the ZC0.3-Ag coating (Fig. 2) revealed an uneven and rough surface. The crystal structure and chemical composition of the coating were further investigated with TEM. The bright-field TEM image of the ZC0.3-coating is shown in Fig. 3a. The selected-area diffraction (SAED) pattern (Fig. 3b) of the encircled area indicated the presence of a crystalline $Ca_2ZnSi_2O_7$ phase with a zone axis of [1 $\overline{3}$ $\overline{2}$]. The energy disperse spectroscopy (EDS) analysis (Fig. 3c) of the encircled area showed the presence of calcium, silicon and zinc, further confirming the presence of the crystallized $Ca_2ZnSi_2O_7$ phase. Several round dark nanoparticles can also be observed in Fig. 3a. A high-magnification view of the black selected area is displayed in Fig. 3d. Dark nanoparticles 10–100 nm in diameter were randomly distributed in the glassy matrix, which was confirmed by the SAED pattern (Fig. 3e) of a typical amorphous phase. The SAED pattern (Fig. 3f) of the nanoparticle indicated the presence of crystalline Ag with a zone axis of [0 $\overline{1}$ $\overline{1}$]. A high-resolution electron microscopy (HREM) image of the nanoparticle revealed that the lattice spacing matched the fcc Ag (111) plane. A typical EDS analysis with the electron beam focused on one Ag nanoparticle is shown in Fig. 3g, confirming that the nanoparticles are nanocrystalline silver.

The XPS measurements of the ZC0.3-Ag coating surface were carried out, and the feature peak of Ag $3d_{5/2}$ can be detected in Fig. 4. The peaks were fitted with two doublets using the binding energy (BE) and FHWM values according to the literature data [14]. The peak at 368.0 eV is assigned to metallic Ag^0, whereas the other peak at 368.7 eV corresponds to Ag^+. The detected Ag^+ should be attributed to the formation of Ag_2O on the surface of the silver nanoparticles.

3.2. Chemical stability and Ag^+ release

The mass losses of the as-sprayed coatings after immersion in the Tris-HCl buffer solution are presented in Fig. 5. The mass loss of the Ag-doped calcium silicate coating showed no statistical difference with that of the original coating. Nevertheless, the mass loss of the ZC0.3-Ag coating was much lower than that of the Ag-doped coating. This enhanced chemical durability should be attributed to the formation of the stable $Ca_2ZnSi_2O_7$ phase in the ZC0.3-Ag coating. Fig. 6 shows the amount of silver released from the ZC0.3-Ag coating in Tris-HCl buffer solution as a function of time. Ag^+ was released in an initial burst over the first 7 days of immersion, followed by much slower release over days 7–14. However, after 14 days, the total release of Ag^+ concentration was under 1 ppm.

3.3. Antibacterial activity

The representative macroscopic images of viable bacteria after 24 h of interaction with the ZC0.3-Ag coating and the uncoated Ti–6Al–4V control are shown in Fig. 7. The number of viable bacteria (*S. aureus* and *E. coli*) was significantly reduced on the ZC0.3-Ag coating when compared to that on the uncoated Ti–6Al–4V. The calculated antibacterial ratio of the ZC0.3-Ag coating against *E. coli* and *S. aureus* was as high as 99%.

3.4. Morphology of hMSCs

The initial adhesion and spreading activity of hMSCs cultured on the uncoated Ti–6Al–4V and the ZC0.3-Ag coating for 24 h are shown in Fig. 8. Both of the surfaces were found to be able

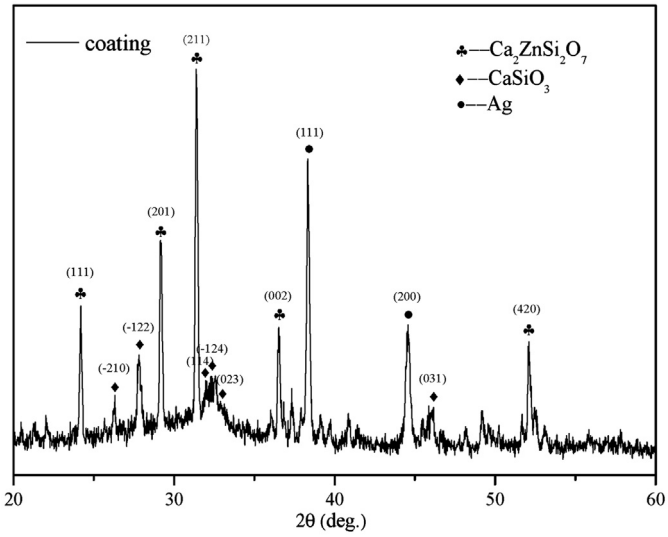

Fig. 1. An XRD pattern of the ZC0.3-Ag coating.

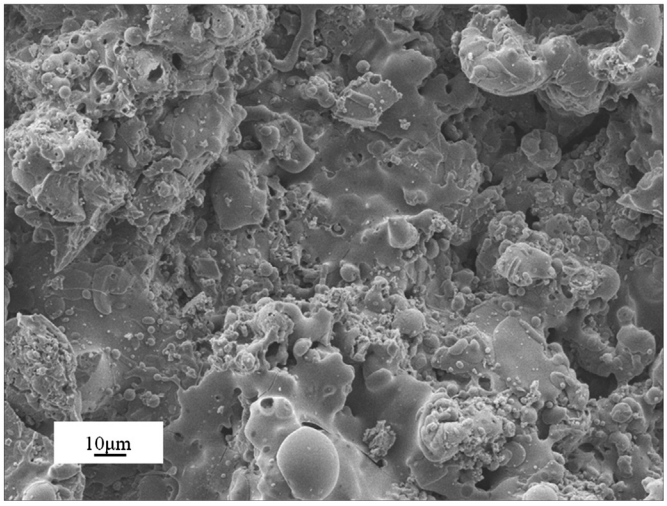

Fig. 2. The surface morphology of the ZC0.3-Ag coating.

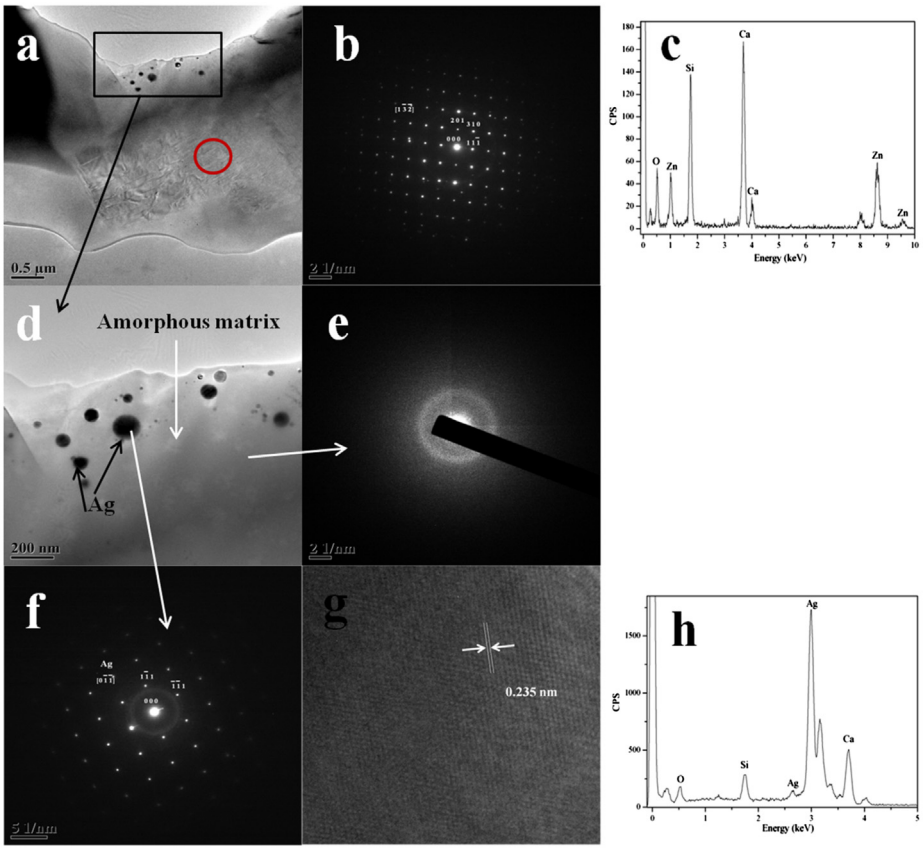

Fig. 3. TEM micrographs of the ZC0.3-Ag coating: (a) a bright-field TEM image; (b) the SAED pattern and (c) the EDS analysis of the area enclosed by the red circle; (d) a high-magnification view of the selected area; (e) the SAED pattern of the smooth matrix; (f) the SAED pattern and (g) an HREM image showing the corresponding lattice spacing and (h) the EDS analysis of one dark nanoparticle. (For interpretation of the references to color in this figure legend, the reader is referred to the web version of this article.)

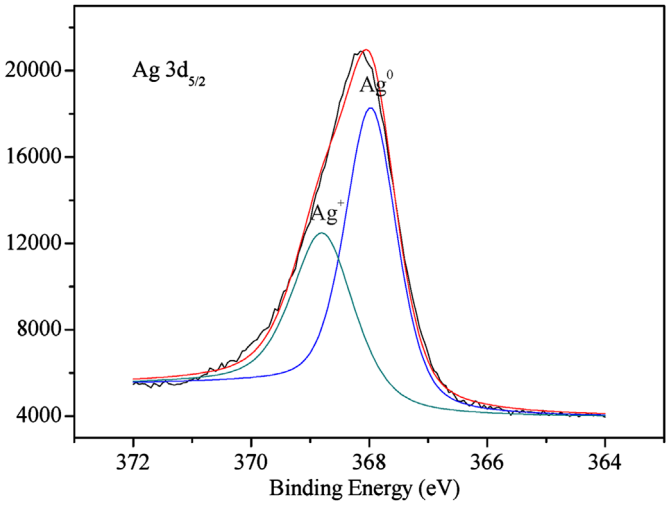

Fig. 4. The XPS spectrum of the Ag $3d_{5/2}$ region in the ZC0.3-Ag coating.

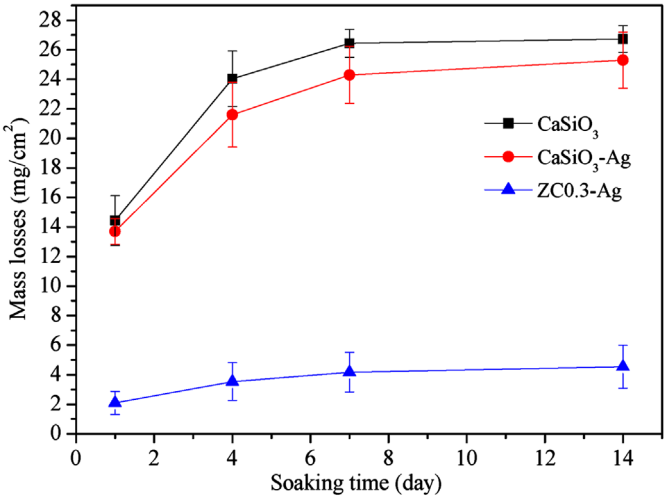

Fig. 5. The mass losses of the $CaSiO_3$, $CaSiO_3$-Ag and ZC0.3-Ag coatings immersed in Tris-HCl buffer solution with time.

to support cell growth. The cells spread well, were in close contact with the surface of the uncoated Ti–6Al–4V, and formed multilayers, as shown in Fig. 8a. In Fig. 8c, the cells on the ZC0.3-Ag coating adopted irregular morphology of the coating surface with thin cytoplasmic digitations and exhibited a lower degree of density compared to the cells on the uncoated Ti–6Al–4V. Fig. 8b and d provide clearer details of the adherence. The cells on both surfaces maintained physical contacts with the

neighboring cells through multiple extensions. However, the cells appeared to adhere more tightly on the uncoated Ti–6Al–4V surface compared to the ZC0.3-Ag coating surface.

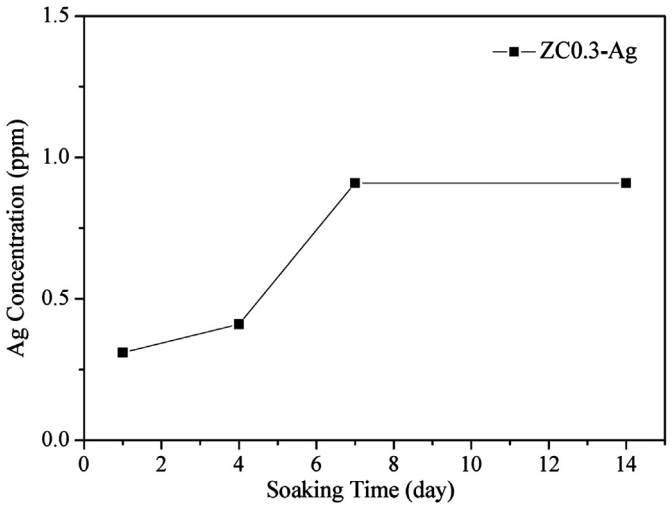

Fig. 6. The Ag^+ released from the ZC0.3-Ag coating immersed in Tris-HCl buffer solution with time.

3.5. Cytotoxicity assessment

The effect of the ZC0.3-Ag coating extracts (prepared at different concentrations) on the proliferation of the hMSCs was examined as shown in Fig. 9. The proliferation of hMSCs increased as the extract concentrations decreased from 2.00 to 0.250 cm^2/ml. The extract at the lowest concentration (0.250 cm^2/ml) showed stimulating effect on the proliferation of the cells when compared with the uncoated Ti–6Al–4V control. However, at the highest concentration (2.00 cm^2/ml), the extract showed significant adverse impacts, which can potentially be attributed to a side effect of adding Ag.

4. Discussion

In the present study, silver was successfully incorporated into the zinc-modified calcium silicate coating and the presence of silver in the coating was confirmed by the XRD, TEM and XPS results. The TEM observations revealed that nanocrystalline silver was mainly found in the amorphous matrix. This phenomenon may result from the molten surface and un-melted core of the particles during the plasma spraying process. It was assumed that the silver nanoparticles formed from the thermal decomposition

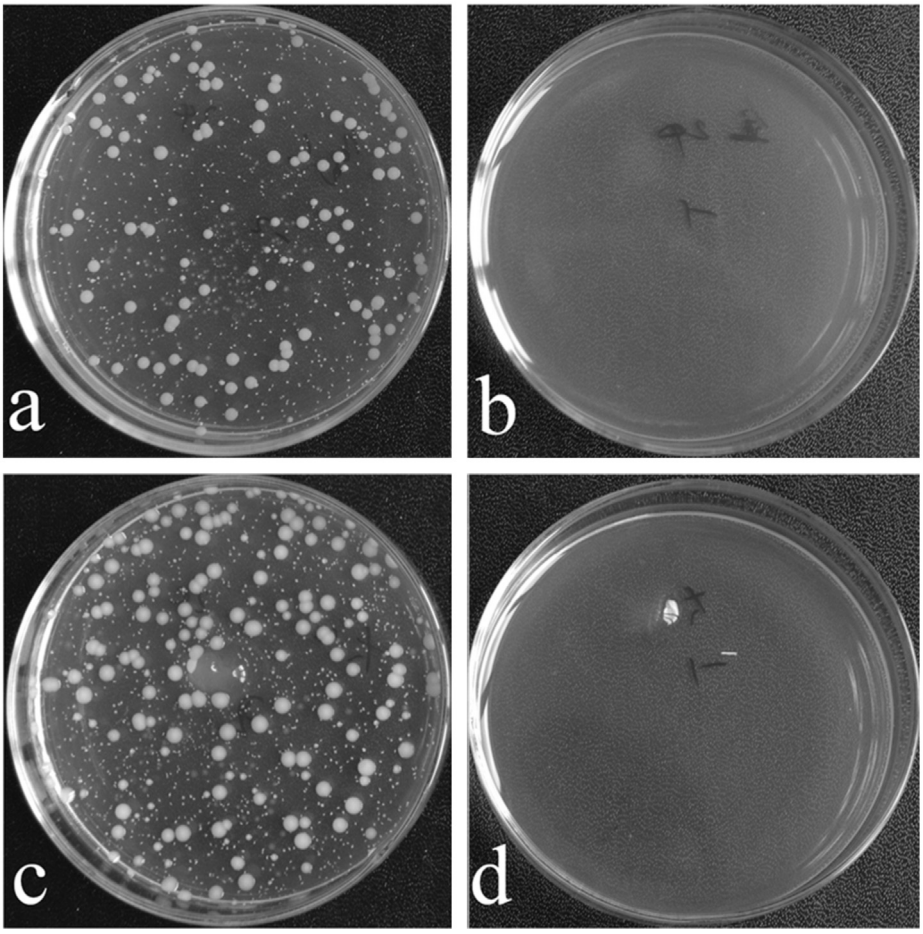

Fig. 7. Representative photos of the viable *E. coli* (b) and *S. aureus* (d) cells after 24 h of interaction with the ZC0.3-Ag coating. Uncoated Ti–6Al–4V (a, c) was used as the control.

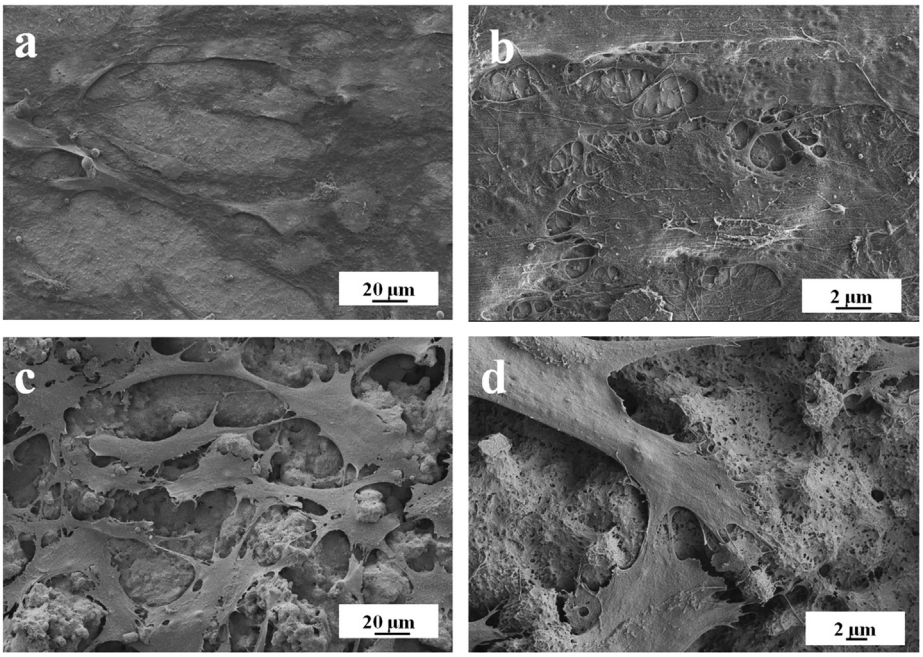

Fig. 8. The SEM images of the hMSCs cultured on the uncoated Ti–6Al—4V (a, b) and the ZC0.3-Ag coating (c, d) for 24 h.

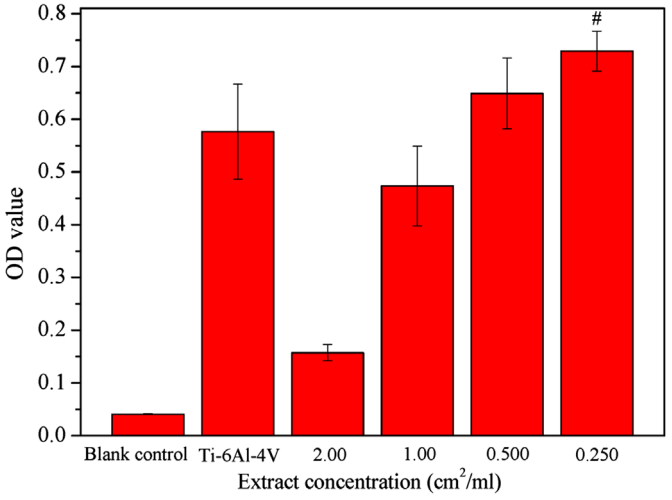

Fig. 9. The cytotoxic evaluation of the ZC0.3-Ag coating extracts at different concentrations. # The experimental group was compared with the uncoated Ti–6Al–4V control group, $p < 0.05$.

of $AgNO_3$ were embedded in other particles during the powder calcination process. Because of the rapid heating/rapid cooling and solidification of the semi-molten particles during the plasma spraying process, the outer layers of these semi-molten particles showed a smooth glassy appearance, whereas their cores, the silver nanoparticles, retained their original texture and structure.

The addition of silver significantly enhanced the bactericidal effect of the Zn-modified coating without compromising the chemical stability. In the chemical durability test, the ZC0.3-Ag coating presented good chemical stability comparable to that of the Zn-modified coating (the data for the Zn-modified coating was included in our previous study). In the present in vitro antibacterial study, the ZC0.3-Ag coating exhibited enhanced bactericidal activity against both the Gram-negative bacteria *E. coli* and the Gram-positive bacteria *S. aureus* compared to the Zn-doped coatings studied in our previous work. The enhanced inactivation of bacteria should be attributed to the presence of Ag nanoparticles in the coating. It has been reported that silver nanoparticles demonstrated excellent antibacterial activity when compared with the other available silver antibacterial agents such as silver sulfadiazine or silver nitrate because the silver nanoparticles release both Ag^+ and other silver species such as Ag^0 [15].

The presence of metallic silver on the surface of the ZC0.3-Ag coating was confirmed by XPS, indicating that there may be Ag nanoparticles present on the surface. Assuming that Ag nanoparticles are present in the coating surface, the inhibitory mechanisms of the ZC0.3-Ag coating are suggested to be as follows. The first is the close contact of the bacteria with the Ag nanoparticles present on the coating surface. The Ag nanoparticles can directly interact with the bacteria, causing the degradation of the lipopolysaccharide molecules in the bacterial membrane and forming "pits" that lead to large increases in membrane permeability. These can prevent bacterial multiplication and/or kill bacteria. [16] The second is the slow release of Ag^+ or the detachment of Ag nanoparticles from the coating into the medium. The Ag nanoparticles or Ag^+ attach to the cell membrane and also penetrate inside the bacteria. These species preferably interact with the sulfur-containing proteins in the cell as well as with phosphorus-containing compounds such as DNA, finally leading to cell death [17,18]. In this work, Ag^+ was released from the coating in an initial burst over the first 7 days of immersion in a Tris-HCl buffer solution. This may stem from the Ag nanoparticles on the surface, which will oxidize when reacting with water. Ag^+ was released at a much slower rate over 7–14 days, and after 14 days, the total released Ag^+ concentration was

under 1 ppm, which is less than the cytotoxic amount (1.6 ppm) as reported [19].

Not only did the addition of silver enhance the bactericidal effect, but the cytocompatibility of the coating was also maintained after silver modification. Cell adhesion and cytotoxicity assays were performed in our work. The ZC0.3-Ag coating was found to support cell growth and adhesion, although the density of hMSCs on the coating was slightly less than that on the uncoated Ti–6Al–4V control. The cytotoxicity evaluation revealed that, at the highest concentration (2.00 cm^2/ml), the ZC0.3-Ag coating extract induced toxicity in cells, which was likely due to a side effect of the silver, but the number of cells in the ZC0.3-Ag coating extract at other concentrations was similar to or higher than that of the uncoated Ti–6Al–4V control extract. Overall, it was concluded that the addition of Ag did not significantly compromise the cytocompatibility of the coating. The toxicology of silver-loaded biomaterials has been widely investigated. Song et al. showed that the silver-containing calcium phosphate coatings at high silver concentrations exhibited cytotoxicity, which was not found for coatings at a low silver concentration [20]. Tweden et al. [21] reported that there was no evidence of silver toxicity for the fibroblast cell line until the concentrations reached 1200 ppb. There is recent evidence suggesting that the potential toxicity of silver nanoparticles to human cells is through reactive oxygen species (ROS) [15,22,23]. Although the previously reported toxicity-induced critical concentrations are higher than the released Ag^+ concentration of the ZC0.3-Ag coating in this work, it is still necessary to optimize the amount of silver in the coating and tailor the release of silver in our future work.

5. Conclusions

In this work, Ag was successfully incorporated into plasma sprayed Zn-modified calcium silicate coating. The presence of metallic silver in the coating was confirmed by the XRD, TEM and XPS results. The silver nanoparticles were randomly distributed in the amorphous matrix, with sizes ranging from 10 to 100 nm. The ZC0.3-Ag coating presented good chemical stability comparable to that of the Zn-modified coating. The addition of Ag significantly enhanced the bactericidal effect of the Zn-modified coating, which was attributed to the Ag nanoparticles present on the surface of the coating. Moreover, the ZC0.3-Ag coating supported the adhesion and spreading of hMSCs on the surface without inducing significant toxicity to the cells.

Acknowledgments

This work was supported by the National Natural Science Foundation of China (Grant nos. 81071455, and 51172264) and the Foundation of Shanghai Biomaterial and Clinic Research Centre (Grant no. BMCRC2010004).

References

[1] R.O. Darouiche, Current concepts—treatment of infections associated with surgical implants, New England Journal of Medicine 350 (2004) 1422–1429.
[2] E.M. Hetrick, M.H. Schoenfisch, Reducing implant-related infections: active release strategies, Chemical Society Reviews 35 (2006) 780–789.
[3] L.W. Duran, Preventing medical device related infections, Medical Device Technology 11 (2000) 14–17.
[4] K.F. Huo, L.Z. Zhao, H.R. Wang, L.Y. Cui, W.R. Zhang, H.W. Ni, Y.M. Zhang, Z.F. Wu, P.K. Chu, Antibacterial nano-structured titania coating incorporated with silver nanoparticles, Biomaterials 32 (2011) 5706–5716.
[5] B.E. Li, X.Y. Liu, F.H. Meng, J. Chang, C.X. Ding, Preparation and antibacterial properties of plasma sprayed nano-titania/silver coatings, Materials Chemistry and Physics 118 (2009) 99–104.
[6] L.Z. Zhao, P.K. Chu, Y.M. Zhang, Z.F. Wu, Antibacterial coatings on titanium implants, Journal of Biomedical Materials Research Part B 91B (2009) 470–480.
[7] Y.K. Chen, X.B. Zheng, Y.T. Xie, C.X. Ding, H.J. Ruan, C.Y. Fan, Antibacterial and cytotoxic properties of plasma sprayed silver-containing HA coatings, Journal of Materials Science: Materials in Medicine 19 (2008) 3603–3609.
[8] A. Travan, E. Marsich, I. Donati, M. Benincasa, M. Giazzon, L. Felisari, S. Paoletti, Silver-polysaccharide nanocomposite antimicrobial coatings for methacrylic thermosets, Acta Biomaterials 7 (2011) 337–346.
[9] Y.F. Zheng, B.B. Zhang, B.L. Wang, Y.B. Wang, L. Li, Q.B. Yang, L.S. Cui, Introduction of antibacterial function into biomedical TiNi shape memory alloy by the addition of element Ag, Acta Biomaterials 7 (2011) 2758–2767.
[10] K. Li, J.M. Yu, Y.T. Xie, L.P. Huang, X.J. Ye, X.B. Zheng, Chemical stability and antimicrobial activity of plasma sprayed bioactive Ca_2Zn-Si_2O_7 coating, Journal of Materials Science: Materials in Medicine 22 (2011) 2781–2789.
[11] K. Li, Y.T. Xie, L.P. Huang, H. Ji, X.B. Zheng, Antibacterial mechanism of plasma sprayed $Ca_2ZnSi_2O_7$ coating against Escherichia coli, Journal of Materials Science: Materials in Medicine (2012).
[12] H. Tapiero, K.D. Tew, Trace elements in human physiology and pathology: zinc and metallothioneins, Biomedicine and Pharmacotherapy 57 (2003) 399–411.
[13] S. Samani, S.M. Hossainalipour, M. Tamizifar, H.R. Rezaie, In vitro antibacterial evaluation of sol–gel-derived Zn-, Ag-, and (Zn + Ag)-doped hydroxyapatite coatings against methicillin-resistant *Staphylococcus aureus*, Journal of Biomedical Materials Research Part A (2012).
[14] S.M. Magana, P. Quintana, D.H. Aguilar, J.A. Toledo, C. Angeles-Chavez, M.A. Cortes, L. Leon, Y. Freile-Pelegrin, T. Lopez, R.M.T. Sanchez, Antibacterial activity of montmorillonites modified with silver, Journal of Molecular Catalysis A: Chemical 281 (2008) 192–199.
[15] K. Chaloupka, Y. Malam, A.M. Seifalian, Nanosilver as a new generation of nanoproduct in biomedical applications, Trends Biotechnology 28 (2010) 580–588.
[16] B.S. Necula, J.P.T.M. van Leeuwen, L.E. Fratila-Apachitei, S.A.J. Zaat, I. Apachitei, J. Duszczyk, In vitro cytotoxicity evaluation of porous TiO_2-Ag antibacterial coatings for human fetal osteoblasts, Acta Biomaterials 8 (2012) 4191–4197.
[17] D.R. Monteiro, L.F. Gorup, A.S. Takamiya, A.C. Ruvollo, E.R. Camargo, D.B. Barbosa, The growing importance of materials that prevent microbial adhesion: antimicrobial effect of medical devices containing silver, International Journal of Antimicrobial Agents 34 (2009) 103–110.
[18] W.R. Li, X.B. Xie, Q.S. Shi, H.Y. Zeng, Y.S. Ou-Yang, Y.B. Chen, Antibacterial activity and mechanism of silver nanoparticles on *Escherichia coli*, Applied Microbiology and Biotechnology 85 (2010) 1115–1122.
[19] N. Rameshbabu, T.S.S. Kumar, T.G. Prabhakar, V.S. Sastry, K.V.G.K. Murty, K.P. Rao, Antibacterial nanosized silver substituted hydroxyapatite: Synthesis and characterization, Journal of Biomedical Materials Research Part A 80A (2007) 581–591.
[20] W.H. Song, H.S. Ryu, S.H. Hong, Antibacterial properties of Ag (or Pt)-containing calcium phosphate coatings formed by micro-arc oxidation, Journal of Biomedical Materials Research Part A 88 (2009) 246–254.

[21] K.S. Tweden, J.D. Cameron, A.J. Razzouk, W.R. Holmberg, S.J. Kelly, Biocompatibility of silver-modified polyester for antimicrobial protection of prosthetic valves, Journal of Heart Valve disease 6 (1997) 553–561.

[22] Y.H. Hsin, C.F. Chen, S. Huang, T.S. Shih, P.S. Lai, P.J. Chueh, The apoptotic effect of nanosilver is mediated by a ROS- and JNK-dependent mechanism involving the mitochondrial pathway in NIH3T3 cells, Toxicology Letters 185 (2009) 142-142.

[23] C. Carlson, S.M. Hussain, A.M. Schrand, L.K. Braydich-Stolle, K.L. Hess, R.L. Jones, J.J. Schlager, Unique cellular interaction of silver nanoparticles: size-dependent generation of reactive oxygen species, J. Phys. Chem. B 112 (2008) 13608–13619.